Are there bipolarons in icosahedral boron-rich solids?

2007 J. Phys.: Condens. Matter 19 186207

(http://iopscience.iop.org/0953-8984/19/18/186207)

IOP PUBLISHING JOURNAL OF PHYSICS: CONDENSED MATTER

J. Phys.: Condens. Matter **19** (2007) 186207 (14pp) doi:10.1088/0953-8984/19/18/186207

Are there bipolarons in icosahedral boron-rich solids?

H Werheit

Institute of Physics, University Duisburg-Essen, Campus Duisburg, D-47048 Duisburg, Germany

E-mail: helmut.werheit@uni-duisburg-essen.de and helmut.werheit@koeln.de

Received 4 October 2006, in final form 8 March 2007
Published 5 April 2007
Online at stacks.iop.org/JPhysCM/19/186207

Abstract

The charge transport of boron carbide, often incorrectly denoted as B_4C, has been controversially discussed. It is shown that the bipolaron hypothesis is not compatible with numerous experimental results. In particular, the determined real microstructure of boron carbide and its related electronic properties disprove several assumptions, which are fundamental to the bipolaron hypothesis. In contrast, the actual energy band scheme derived mainly from optical investigations is confirmed by careful evaluation of the high-temperature electrical conductivity, and allows a consistent description at most of the experimental results.

1. Introduction

Icosahedral boron-rich solids are very promising candidates for high-efficiency thermoelectric energy conversion [1]. Nevertheless, many of their solid state and semiconducting properties have remained unsolved. One important open question is the charge transport, which has been controversially discussed. Essentially, two models remain. The bipolaron model created by Emin and co-workers is based on since disproved idealized crystal structures, which, according to theoretical band structure calculations, exhibit high electron deficiencies in the valence bands. These holes are assumed to generate bipolarons (e.g. in $B_{11}C$ icosahedra of boron carbide) being decisive for the charge transport in these complex structures. In contrast, the concept developed by Werheit and co-workers requires that the results of theoretical band structure calculations based on idealized crystal structures are modified to account for of the real structure of these solids. High-density intrinsic structural defects exactly compensate the calculated valence electron deficiency by generating corresponding densities of split-off valence states in the gap. The charge transport is due to hopping processes within these partially filled gap states, superimposed by a certain contribution from free holes, whose share depends, for example, on thermal or optical excitation of valence electrons into these gap states.

Recently [2], Emin resurrected the hypothesis of small bipolarons in icosahedral boron-rich structures, in particular in boron carbide, developed in [3–8] without taking into account the numerous conflicting experimental results. Theoretical models require confirmation by

Table 1. Concentration of structural elements in the elementary cell of boron carbide at some selected chemical compositions within the homogeneity range [16, 23, 24, 21, 22, 40].

	$B_{4.3}C$	$B_{13}C_2$	B_8C
B_{12} icosahedra	0	42	26
$B_{11}C$ icosahedra	100	58	74
C–B–C	81	62	7
C–B–B	19	19	77
B–□–B (□, vacancy)	0	19	16

experiment. In this respect the author appealed to the small number of ESR centres measured in boron carbide compared to an assumed high concentration of carriers in the valence band, and to a satisfactory fitting of the temperature dependences of the electrical conductivity and Seebeck coefficient.

The bipolaron model is essentially based on the discrepancy between a hypothetically assumed high concentration of carriers ($\sim 10^{21}$ cm^{-3}) and the numerous experimental results of different authors (ESR, transport) consistently proving carrier concentrations of the order of $\sim 10^{19}$ cm^{-3} for boron carbide. However, this high concentration of carriers was substantiated by inappropriate assumptions about the microstructure. The calculated electron deficiency of the order of $\sim 10^{21}$ cm^{-3} in boron carbide (see e.g. [9–12]) characterizes it as a metal in contrast to its real semiconducting character, and this electron deficiency was taken as the number of free holes. However, as shown in [13, 14], in real of icosahedral boron-rich structures there are high concentrations of intrinsic structural defects exactly compensating the theoretically calculated electron deficiencies. Accordingly, the real valence bands are completely filled, and hence these solids are semiconductors in accordance with experiment. The real structures do not justify the assumption of such high carrier concentrations in the valence bands. Accordingly, this fundamental prerequisite for the bipolaron model is absent.

2. Homogeneity range and microstructure of boron carbide

The homogeneity range of boron carbide, often incorrectly denoted as B_4C, extends from $B_{4.3}C$ at the carbon-rich limit to $B_{\sim 11}C$ at the boron-rich limit. The carbon-rich limit was proved by Schwetz and Karduck [15] for the first time, and has since been confirmed by numerous other investigators (see e.g. [16], figure 254, and assigned references). Leithe-Jasper and Tanaka [17] (see [18]) realized that $B_{4.3}C$ is the only boron carbide composition that allows the growth of single crystals. The compound B_4C does not exist. If this chemical composition is obtained, it consists of the compound $B_{4.3}C$ and precipitated graphitic free carbon. Therefore, in particular close to the carbon-rich limit of the homogeneity range, for a reliable chemical analysis of boron carbide a separate analysis of bonded and free carbon in the structure is indispensable [19]. $B_{11.2}C$ synthesized by Gosset and Colin [20] seems to be the boron carbide with the lowest carbon content hitherto obtained.

Meanwhile, the quantitative concentration of the different structural elements of boron carbide has been determined for the whole homogeneity range by the evaluation of IR and Raman active phonon spectra (see [16, 21–24]). Some of the results are listed in table 1. Some uncertainty remains close to the boron-rich limit, caused by the weak IR phonon bands.

The concentration of vacancies in the centre of the unit cell was confirmed by neutron diffraction experiments [25]. In a recent NMR analysis of 'B_4C' (probably $B_{4.3}C$) [26] it was established that there are no C–C–C chains. However, Raman investigations on isotope-enriched boron carbide [24] indicate that apparently the existence of small concentrations of

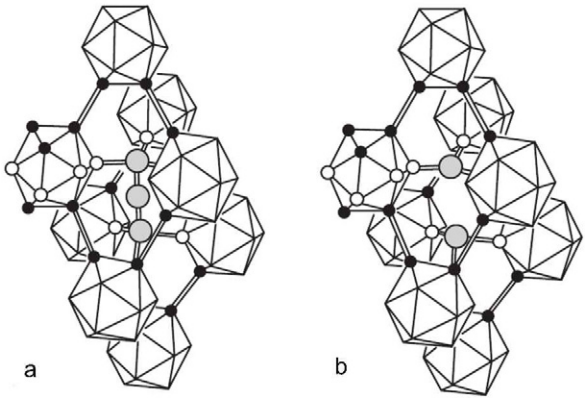

Figure 1. Boron carbide structure consisting of elementary cells statistically composed of B_{12} and $B_{11}C$ icosahedra on the vertices, and (a) three-atomic (C–B–C, C–B–B) or (b) two-atomic (B–□–B (□, vacancy)) linear arrangements on the main diagonal of the rhombohedral cell. The concentrations of the structural elements depend on the actual chemical composition.

C–C–C chains cannot be excluded under as yet undefined preparative conditions. The C atoms in the icosahedra reside on polar sites only; this conclusion [27] was recently confirmed [26]. The assumption that there are about 2.5% $B_{10}C_2$ icosahedra [26] is not supported by the phonon spectra but could be below the detection limit.

In boron carbide there is no unit cell representing the whole structure, which is composed of nearly isomorphous elementary cells whose microstructures vary (figure 1). Their conformity is 12-atomic, by the Jahn–Teller effect slightly distorted icosahedra at each vertex, and the mostly three-atomic linear chains on the main diagonal parallel to the crystallographic *c*-axis. B_{12} and $B_{11}C$ icosahedra, C–B–C, C–B–B, B–□–B (□, vacancy), form differently composed elementary cells, statistically distributed over the whole structure (see [16] and references therein, [24, 23]). The poorly defined occupation of specific atomic sites by B and C atoms, together with their very similar x-ray scattering cross sections, are responsible for the failure of such investigations to determine structural details.

Schmechel and Werheit [13, 14] proved that these intrinsic structural defects generate split-off valence states in the band gap, which exactly compensate the electron deficiency calculated for the hypothetical structure formula B_{12} C–B–C [9–12]. Real $B_{13}C_2$ boron carbide exhibits the extraordinary high concentration of 0.97(5) intrinsic point defects per unit cell [13, 14] accompanied by a strong average distortion of the whole structure [27]. This easily explains the very low thermal conductivity of boron carbide. In figure 2 the concentrations of the structural elements in boron carbide are displayed in (a), and the related electronic compensation of the electron deficiency calculated in comparison to the hypothetical B_{12} C–B–C structure in (b).

The concentrations of the different structural elements in the elementary cells of boron carbide within the homogeneity range were determined by fitting atom and isotope-dependent models of the microstructure to specific related lattice vibrations in the IR absorption and the FT-Raman spectra (FT, Fourier transform) of natural, ^{10}B and ^{11}B enriched boron carbide of various compositions [21–24]. The reliability of the FT-Raman spectra of boron carbide used for this evaluation, in contrast to the conventional Raman spectra published by some other authors, has been carefully proved [28].

The substitution of C for B in the $B_{11}C$ icosahedra of boron carbide generates one donor each and accordingly supplies one excess electron to the idealized B_{12} C–B–C structure. According to theoretical calculations [11, 12], in this way the valence electron deficiency

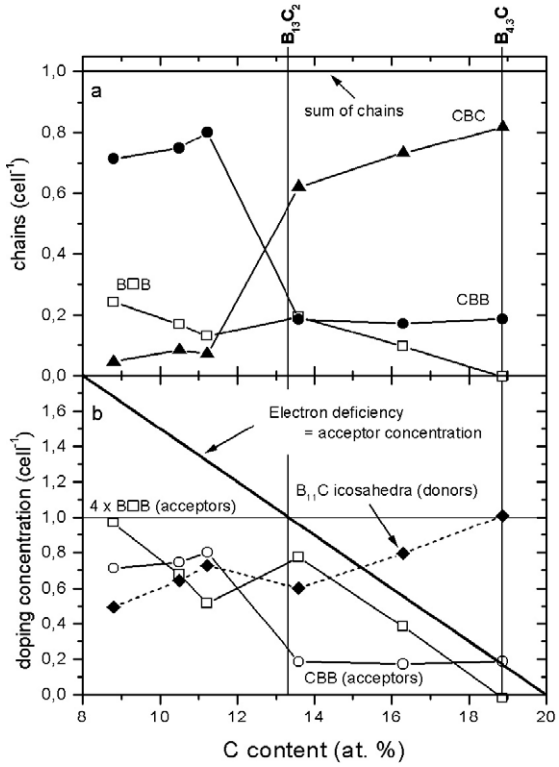

Figure 2. Boron carbide. (a) Chain concentrations within the homogeneity range. (b) Compensation of the theoretical electron deficiency (for hypothetical B_{12} C–B–C, the deficiency is one electron; for hypothetical $B_{12}C_3$, zero electrons per unit cell) in the real structures. C–B–B generates one acceptor, B–□–B generates four acceptors; the $B_{11}C$ icosahedron generates one donor (for details, see [13, 14]).

of the hypothetical B_4C (($B_{11}C$) C–B–C) structure is exactly compensated. However, in the real boron carbide structure close to the carbon-rich limit of the homogeneity range a certain compensation by structural defects takes place as well. Accordingly, after the valence band of these compounds has been completely filled by electrons coming from the $B_{11}C$ icosahedra as donors, a certain portion of excess electrons remains for occupying acceptor sites in the gap generated, for example, by C–B–B and B–□–B defects. These electrons are responsible for the hopping type conductivity.

3. Effective mass, Raman effect, electron–phonon coupling

(Bi)polarons are quasiparticles generated by self-trapping of sufficiently slowly moving charge carriers polarizing immediately neighbouring structural elements. The mobility of the charge carriers is additionally reduced because they have to carry their polarized surroundings with them. Accordingly, on one hand the formation of (bi)polarons is favoured by a high effective band mass of the carriers, and on the other hand a high polarizability of the structural elements and a high electron–phonon interaction, respectively, is required.

The problem of the effective mass of the band carriers is a central one in (bi)polaron physics (see e.g. [29]). Emin's model is based on the formation of small (bi)polarons

in $B_{11}C$ icosahedra; their mass would be considerably higher than the band mass of free holes. Unfortunately, reliable experimental effective mass values for boron carbide like those, which can be obtained for example by cyclotron resonance experiments, are not available. Accordingly, the discussion must be restricted to more or less rough estimations. The band mass of free holes in boron carbide $m_p \sim 10\ m_0$ estimated from the curvature of theoretical band structure calculations [9] was found to agree with the experimental value obtained from luminescence [51]. The effective masses estimated for mobile carriers from electrical conductivity and ESR ($m^* > 3\ m_0$) [30], from IR spectra ($m^* \sim 3$–$5\ m_0$, $m^* \sim 10\ m_0$) [31, 32], and from the dynamical conductivity ($m^* \sim 1$–$10\ m_0$) [34, 35] could be assigned to the (bi)polarons. However, obviously there is no indication that the effective mass of the mobile carriers in boron carbide is considerably larger than the band mass of free holes. Hence these results disagree with the small polaron model.

The weak IR phonons indicate largely covalent bonding in icosahedral boron-rich solids. A direct measure for the polarizability is the strength of the Raman effect. Compared with other covalently bonded solids, the Raman effect of icosahedral boron-rich solids is extraordinarily weak. This is indicated by the very long integration times needed for sufficiently resolved Raman spectra, far exceeding those for other covalent solids (see, e.g., references in [16]). For example, the FT-Raman spectra of boron carbide presented in [21–24] required integration times of up to 6 h, while with the same equipment about 20 s were sufficient for spectra of other covalent crystals with a similar signal-to-noise ratio. Such extremely small polarizabilities make the formation of bipolarons in icosahedral boron-rich solids improbable at the very least.

Calandra *et al* [33] confirmed this conclusion, arguing that the moderate electron–phonon coupling $\lambda = 0.81$ is too small to justify a bipolaronic state for $B_{13}C_2$.

4. Composition-dependent electrical conductivity in boron carbide

According to Emin *et al* [3–8] electronic transport in boron carbides proceeds via hopping of bipolarons between $B_{11}C$ icosahedra. This model is based on a calculated energy reduction of ~16.5 eV for adding two electrons to a $B_{11}C$ icosahedron compared with ~3.7 eV for the B_{12} icosahedron.

This assumption was checked in [34, 35]. For dc electrical conductivity the density of hopping sites was determined according to Mott's law of variable-range hopping $\sigma = \sigma_0 \exp[-(T_0/T)^{1/4}]$ (σ_0 and T_0 are fitting parameters to the experiment) [36]. For the dynamical conductivity the density of hopping sites n_s was obtained from the factor $A \propto n_s^2 T$ in $\sigma(\omega) = A \int_0^\infty [x^4/[e^x + i(\omega_\tau/\omega)]]\,dx$ (ω_τ being the scattering frequency of Drude-type carriers) (see table 1), following the theory of Butcher and Morris [37] (the applicability of this theory is discussed in [34]). Figure 3 shows that the shape of densities of hopping sites is satisfactorily compatible for dc and dynamical conductivity within the homogeneity range of boron carbide; however, it is opposite to the concentration of the $B_{11}C$ icosahedra. Thus this aspect of the bipolaron hypothesis is disproved.

5. High-temperature electrical conductivity of boron carbide

In figure 4 the high-temperature electrical conductivity of a 'typical boron carbide' taken by Emin [3, 7, 8] for adapting the bipolaron theory is compared with some selected experimental data measured by different groups [36, 38, 43] (see also [16]). The qualitative deviation is obvious.

There are several temperature ranges characterized by different thermal activation energies displayed in figure 5 as determined for various boron carbides within the homogeneity range using original data [36, 43] or data reproduced from the literature [38].

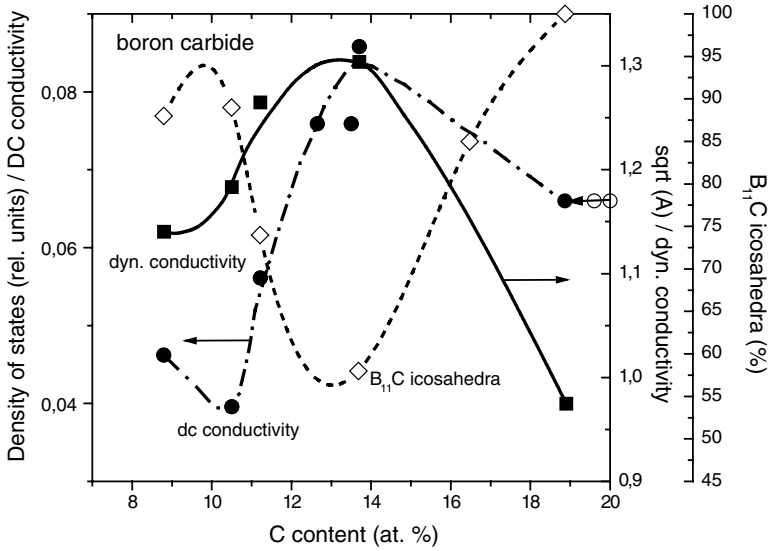

Figure 3. Boron carbide. Experimentally determined densities of hopping sites compared with the density of B_{12} icosahedra versus carbon content: ●, derived from DC conductivity according to Mott's law for variable-range hopping ('B_4C' results have been shifted to $B_{4.3}C$); ○, DC results shifted to the carbon-rich limit of the homogeneity range; ■, full line, sqrt (A) ∝ density of hopping sites derived from dynamical conductivity results (FIR); ◇, dashed line, density of $B_{11}C$ icosahedra (data connected by a spline function).

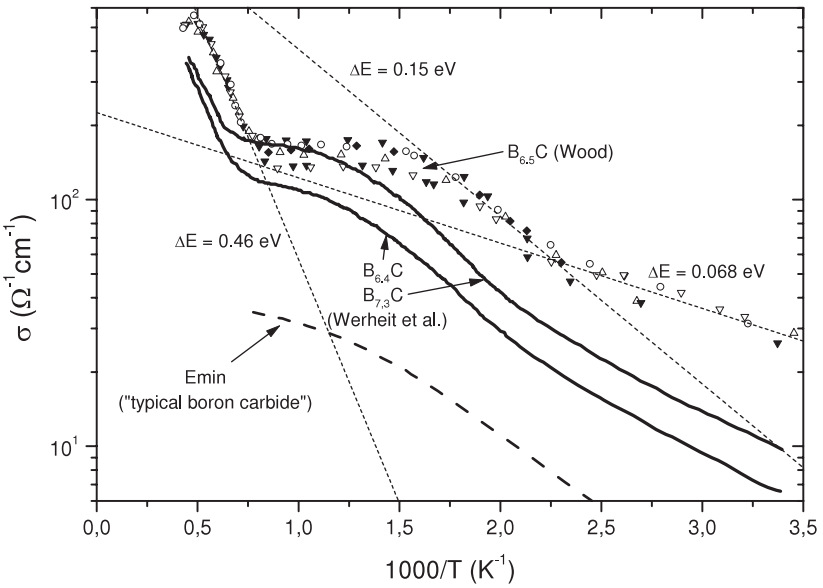

Figure 4. Boron carbide. High-temperature electrical conductivity: dashed curve, 'typical boron carbide', [3, 7, 8]; symbols [38]; solid curves, [36, 43]; short-dashed curves, fits for determining the activation energies.

The activation energies agree well with the transition energies determined by decomposing the optical absorption edge (see below, figure 8). Obviously, up to about 400 K the Fermi

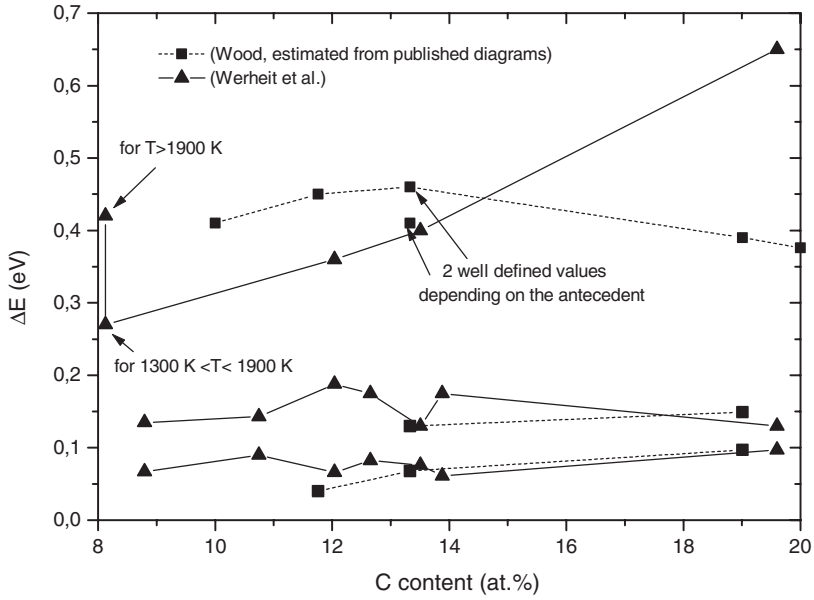

Figure 5. Boron carbide. Thermal activation energies of the electrical conductivity at high temperatures: ■, estimated from diagrams published by Wood [38]; ▲, obtained from original data [36, 43].

level is positioned within the acceptor level, 0.065 eV above the valence band edge. When the thermal activation is sufficiently high, it is shifted to the 0.18 eV level, where it remains between 400 and 580 K. Between 1150 and 1800 K it is pinned in the 0.47 eV level. In these ranges the conductivity increases because of the thermal generation of further free holes by the thermal excitation of electrons into the particular gap states. In the intermediate ranges the electrical conductivity only weakly depends on temperature because the thermal energy is not sufficient to excite electrons into the next level. Such an intermediate range is also indicated at the high-temperature end of Wood's results between 2000 and 2400 K. This makes it clear that below the melting point of about 2600 K in boron carbide no essential intrinsic conductivity with thermal excitation across the band gap can be expected. This is confirmed by the Seebeck coefficient of boron carbide, which is positive and monotonically increases at a high level up to temperatures of at least 2000 K (see [1, 16]). There seems to be no essential difference for boron carbides of different compositions within the homogeneity range. This is not surprising, because not the kind but only the concentration of structural defects (see table 1 and figure 2) depends on the actual compound.

6. Charge transport in icosahedral boron-rich solids

After Emin [39], the coherent motion of bipolarons yields Drude-like optical spectra at low temperatures decreasing with increasing temperatures. The experimental finding is opposite to this prediction.

The dynamical conductivity of numerous icosahedral boron-rich solids was derived from IR spectra between 10 and 5000 cm^{-1} for temperatures between 90 and 450 K [34, 35, 41]. The assumption of a superposition of hopping-type and Drude-type carriers allowed a satisfactory fit of the spectra. For boron carbide the parameters are listed in table 2; for temperatures below 300 K the Drude-type share falls below the detection limit.

Table 2. Electronic transport parameters used for fitting the dielectric function [34, 35, 41]: A, the parameter in $\sqrt{A/T}$ (T, temperature), which is proportional to the density of hopping states; ω_p, plasma frequency; ω_τ, scattering frequency of Drude-type carriers.

	Temperature							
	300 K				450 K			
Compound	A (Ω^{-1} cm^{-1})	ω_p (cm^{-1})	ω_τ (cm^{-1})	p (10^{17} cm^{-3})	A (Ω^{-1} cm^{-1})	ω_p (cm^{-1})	ω_τ (cm^{-1})	p (10^{17} cm^{-3})
$B_{10.37}C$	0.65	—	150	—	1.3	90	1100	2.3
$B_{8.52}C$	0.5	30	1100	0.25	1.4	80	1100	1.8
$B_{7.91}C$	0.75	40	1100	0.45	1.6	110	1100	3.4
$B_{6.3}C$	1.5	90	1100	2.3	1.7	200	1100	11.3
$B_{4.3}C$	0.4	—	150	—	0.95	70	1100	1.38

The densities of Drude-type free carriers are calculated according to

$$n = \frac{\omega_p^2 \varepsilon_0 m^*}{e_0^2}$$

with $\varepsilon = 10\varepsilon_0$ and $m^* = 10\, m_0$ [16].

The Drude-type contributions to the dynamical conductivity decrease with decreasing temperature, indicating a thermal activation energy of about 0.15 eV (only roughly estimated because there are values for two temperatures only).

In figure 6 the carrier densities in carbon-rich boron carbides obtained by different experimental methods are compared. The spin density [42] exceeds the Hall density [38, 43] in the whole temperature range. Chauvet *et al* [42] report on a dominant broad Lorentzian ESR line superimposed by a very narrow line, which was neglected because of its low integrated intensity (∼1/400th of the dominant line). Figure 6 shows that the concentration of Drude-type carriers is of this order. Accordingly, we assume that the neglected narrow ESR line probably represents the free holes in the valence band of boron carbide.

In high magnetic fields (up to 15 T) the magnetoresistance of boron carbide indicates the start of Shubnikov–de Haas (SdH) oscillations [44]. Though the experimental range does not yield multiple SdH oscillations, and therefore the data are not sufficient for a precise calculation, the density of carriers can at least be roughly estimated with

$$n = \frac{e}{\pi\hbar}\frac{1}{\Delta(1/B)}$$

where $\Delta(1/B)$ is to be obtained from the positions of two successive extrema of SdH oscillations. The results estimated for 77 and 290 K are of the same order as the concentrations of the Drude-type carriers of the dynamical conductivity.

Taking the $B_{11}C$ icosahedra (one per unit cell for $B_{4.3}C$) for the concentration of donors supplying the electrons, which partly occupy gap states close to the valence band, it is obvious that the spin density determined by Chauvet *et al* [42] is too low to represent the entire population of these states. We agree with the statement of these authors—that this implies the formation of singlets of paired carriers. However, these are not necessarily bipolarons. For the spin densities at temperatures >500 K the thermal activation energy 0.089(3) eV can be determined, indicating that this energy is sufficient to bring electrons paired in a ground state into an excited state, which allows their determination by ESR.

Obviously, without more detailed knowledge of the transport mechanisms of band type and hopping charge carriers, the low-field Hall effect does not yield quantitatively utilizable results.

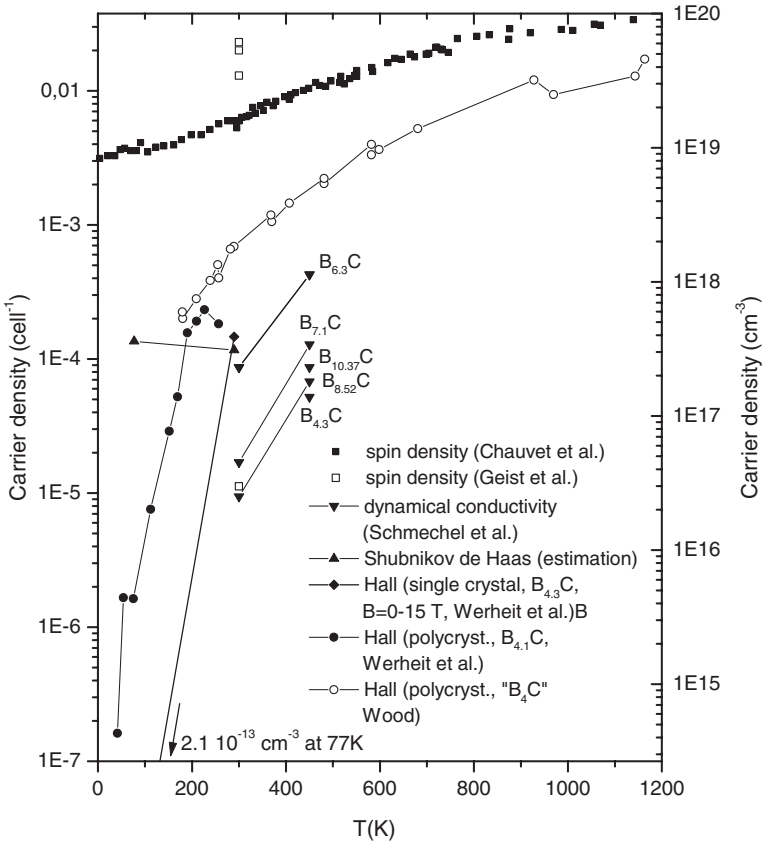

Figure 6. Boron carbide. Comparison of carrier densities determined by different experimental methods: ■, spin density [42]; □, [49, 50] spin densities showing the strong spreading for differently prepared samples of nominally the same composition; properties for comparison; ▼, free hole densities (Drude type), [34, 35]; ▲, free hole density, estimated from SdH oscillations (this work), experimental results [44]; ♦, Hall density measured in high magnetic field ($B = 0$–15 T), [44]; ●, Hall density [43]; ○, Hall density [38].

Accordingly, the existence of (bi)polarons can be excluded for several reasons: (i) The temperature dependence of the experimentally determined Drude-type share of the dynamical conductivity is opposite to that predicted for bipolarons. (ii) The simultaneous existence of bipolarons with the experimentally proved Drude-type free carriers can be excluded. (iii) The measured spin density must be discussed in relation to the conditions in the real solids, and not to a theoretically calculated valence electron deficiency in hypothetical structures (see above).

7. Carrier mobility

7.1. β-rhombohedral boron

As proved by numerous experiments (see [45] and references therein), the charge transport in β-rhombohedral boron consists of two shares: (i) the contribution of a low concentration of free carriers in the valence band excited from partially occupied levels in the band gap close to the valence band, and (ii) hopping processes within the gap states. Both processes occur

simultaneously. Their relative contribution to the conductivity depends on the outer conditions, for example temperature or optical excitation.

Recently, in β-rhombohedral boron the drift mobility of the very small concentration of optically generated untrapped electron–hole pairs was determined ($\mu_{\text{ambipolar}} = 565(120)$ cm^2 V^{-1} s^{-1}) [46]. This value corresponds to carrier mobilities known from typical classical semiconductors, e.g. from holes in silicon. Indeed, because of the high trapping probability this mobility of untrapped carriers is far from being representative for the ensemble of holes in the valence band. High probability trapping processes minimize their average lifetime. Nevertheless, the high mobility of untrapped carriers excludes self-trapping of carriers to (bi)polarons in β-rhombohedral boron.

7.2. Boron carbide

Drift experiments in boron carbide are still unknown. Nevertheless, the conditions are expected to be similar to β-rhombohedral boron; indeed the concentration of gap states is much higher, and therefore the expected trapping probability for free carriers as well. Because of the simultaneously working transport mechanisms, and the lack of knowledge about their share, the classical relation $\mu_{\text{H}} = \sigma \cdot R_{\text{H}}$ does not promise reliable carrier mobilities. In figure 7, typical results reported by different authors are displayed showing spreading results. Nevertheless they exhibit a common tendency. At lower temperatures, the Hall mobility increases with increasing temperature and, above about 500 K it decreases.

The problem of unknown details of the charge transport mechanism is largely avoided by determining the carrier mobility from magnetoresistance according to $\Delta\rho/p \approx (\mu_{\text{B}})^2$ averaging only those carriers really contributing to the effect. For comparison with the Hall mobilities, figure 7 contains such results as well. The most reliable results for $\Delta\rho/\rho$ are obviously those obtained by varying the magnetic fields up to 15 T, because these data allow determination of the coefficient μ with high accuracy. These measurements were performed on a boron carbide single crystal obtained by chance in industrial production (ESK, Elektroschmelzwerk Kempten, Germany). According to the new knowledge about the growth of boron carbide single crystals in the laboratory [17, 18] we assume that the composition is $B_{4.3}C$. The tendency of the mobility, decreasing with increasing temperature, is opposite to that of the Hall mobilities. Surprisingly, the Hall mobility of the single crystal obtained in high magnetic fields confirms this tendency, though it is quantitatively different. It should be noted that this Hall mobility is anomalously signed, indicating hopping processes in an odd-membered structure [47, 48].

The low-field magnetoresistance measurements ($B = 1$ T) confirm the tendency of the high-field results, though at lower values, while the Hall mobilities measured on the same samples show the opposite tendency from those of other authors. Accordingly, the qualitatively different results are caused by the method of measurement and not by the sample properties. The reason why the low-field magnetoresistance is distinctly smaller than the high-field results is unresolved. The anomalous sign of the Hall constant indicating hopping confirms the doubts about the evaluation according to the classical Hall theory. This holds for mobility (figure 7) and carrier concentration (figure 6) as well.

Obviously, near ambient temperatures all mobilities meet near 1 cm^2 V^{-1} s^{-1}. As shown above, the carrier concentrations estimated from the beginning SdH oscillations are compatible with the Drude-type carriers in the dynamical conductivity. This suggests identifying them with those carriers which are responsible for magnetoresistance. It seems that the mobilities derived from magnetoresistance are the most reliable ones, in particular when they are obtained at high fields. The decrease in carrier mobility with increasing temperature fundamentally contradicts the (bi)polaron model.

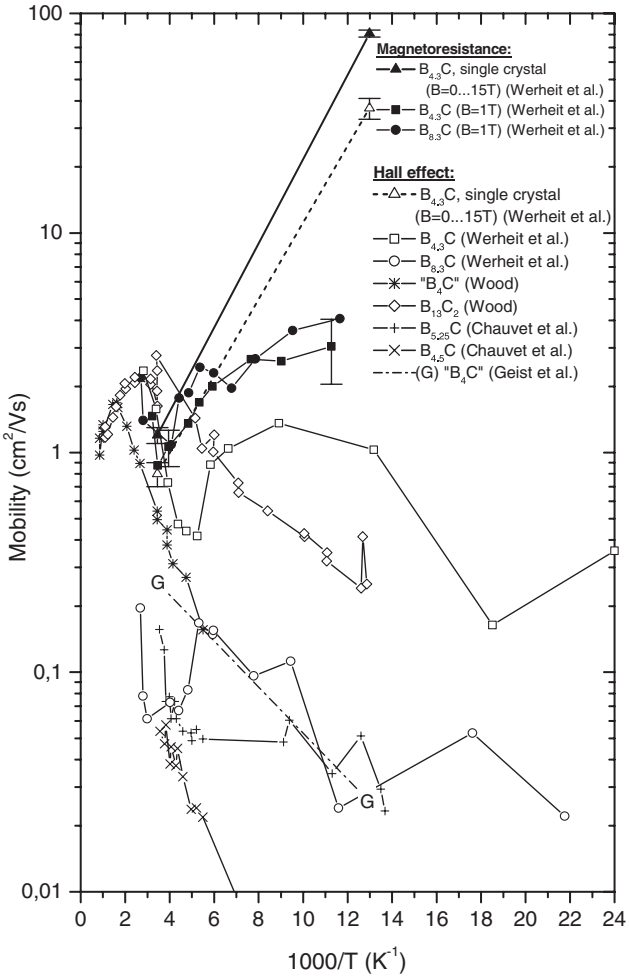

Figure 7. Carrier mobility in boron carbide determined by different experimental methods and authors: ▲, △, [43]; ●, ■, ○, □, Werheit *et al*, partly published in [43]; ∗, ◇, [38]; +, ×, [42]; G — · — G, [49, 50].

8. Excitons

Recently, excitons in boron carbide have been proved in two independent studies [51, 52]. They are associated with the central B atoms in the three-atomic chains, where they exhibit slightly different binding energies for C–B–B and C–B–C [53]. The existence of excitons formed by free carriers is incompatible with the (bi)polaron hypothesis.

9. Band scheme of boron carbide

The actual band scheme of boron carbide is displayed in figure 8.

The position of the deep levels split-off from the valence band was determined by analysing the optical absorption edge [18, 54, 55]. Those at lower energies were satisfactorily confirmed by the activation energies obtained from the electrical conductivity at high temperatures [16, 53]

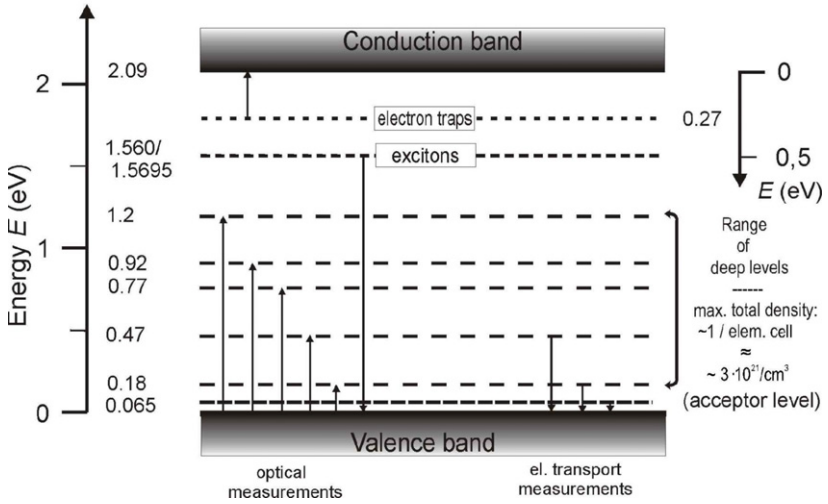

Figure 8. Boron carbide. Energy band scheme based on optical absorption, luminescence, XRS and transport properties. Left ordinate, energies related to the valence band edge; right ordinate, energies related to the conduction band edge. Arrows indicate the direction of the measured transitions.

(see above). The attribution of the 0.47 eV transition determined by optical absorption to a deep level associated with the valence band, and not to the separation of the excitons (∼0.5 eV) from the conduction band is strongly supported by the electrical conductivity confirming this activation energy in a high-temperature range, where the excitons are no longer stable (see [53]).

This band scheme allows a largely consistently description of most of the experimental results hitherto published. Nevertheless, there are numerous problems for understanding the electronic properties which remaining unresolved.

10. Conclusion

The bipolaron hypothesis proved to be incompatible with meaningful experimental results. In particular, the presumed high carrier concentrations were shown to come from incorrect assumptions about the boron carbide microstructure, and the simultaneous existence of bipolarons with the experimentally proved free carriers can be excluded. Accordingly, the bipolaron hypothesis cannot be maintained. This holds at least for β-rhombohedral boron and boron carbide, but with high probability for the other icosahedral boron-rich solids as well.

References

[1] Werheit H 2006 Thermoelectric properties of boron-rich solids and their possibilities of technical application *Proc. 25th Int. Conf. on Thermoelectrics (Vienna, Austria, Aug. 2006)* ed P Rogl (Piscataway, NJ: IEEE) pp 159–63

[2] Emin D 2006 Unusual properties of icosahedral boron-rich solids *J. Solid State Chem.* **179** 2791–8

[3] Emin D 1986 Electronic transport in boron carbides *AIP Conf. Proc.* **140** 189

[4] Howard I A, Beckel C L and Emin D 1987 Bipolaron formation in B_{12} and $(B_{11}C)^+$ icosahedra *MRS Symp. Proc.* **97** 177

[5] Howard I A, Beckel C L and Emin D 1987 Bipolarons in boron icosahedra *Phys. Rev.* B **35** 2929

[6] Howard I A, Beckel C L and Emin D 1987 Bipolarons in boron-rich icosahedra: effect of carbon substitution *Phys. Rev.* B **35** 9265
[7] Emin D 1990 Electronic and vibrational hopping transport in boron carbides *Boron-Rich Solids*; *AIP Conf. Proc.* **231** 65
[8] Emin D 1989 Theory of electronic and thermal transport in boron carbides *The Physics and Chemistry of Carbides, Nitrides and Borides* ed R Freer (Dordrecht: Kluwer) p 691
[9] Armstrong D R, Bolland J, Perkins P G, Will G and Kirfel A 1983 The nature of chemical bonding in boron carbide. IV. Electronic band structure of boron carbide, $B_{13}C_2$, and three models of the structure $B_{12}C_3$ *Acta Crystallogr.* B **39** 324
[10] Armstrong D R 1987 The electronic structure of some α-boron compounds and metal borides *Proc. 9th Int. Symp. on Boron, Borides and Rel. Comp., (Duisburg, Germany)* ed H Werheit (Duisburg: University Press) pp 125–30
[11] Bylander D M, Kleinman L and Lee S 1990 Self-consistent calculations of the energy bands and bonding conditions of $B_{13}C_2$ *Phys. Rev.* B **42** 139
[12] Kleinman L 1991 *Ab initio* calculations of boron and its carbides in boron-rich solids *AIP Conf. Proc.* **231** 13
[13] Schmechel R and Werheit H 1999 Correlation between structural defects and electronic properties of icosahedral boron-rich solids *J. Phys: Condens. Matter* **11** 6803
[14] Schmechel R and Werheit H 1997 Structural defects of some icosahedral boron-rich solids and their correlation with the electronic properties *J. Solid State Chem.* **133** 335
[15] Schwetz K A and Karduck P 1990 Investigations in the boron-carbon system with the aid of electron probe microanalysis *Boron-rich Solids*; *AIP Conf. Proc.* **231** 405–13
[16] Werheit H 2000 Boron compounds *Numerical Data and Functional Relationships in Science and Technology (Landolt–Börnstein New Series* Group III, vol 41D) ed O Madelung (Berlin: Springer) pp 1–491
[17] Leithe-Jasper A and Tanaka T 1999 Crystal growth of boron carbides *13th Int. Symp. on Boron, Borides and Rel. Comp., (Dinard, France, Sept. 1999)* (paper O 22)
[18] Werheit H, Leithe-Jasper A, Tanaka T, Rotter H W and Schwetz K A 2004 Some properties of single-crystal boron carbide *J. Solid State Chem.* **177** 575–9
[19] Schwetz K A and Hassler J 1986 A wet chemical method for the determination of free carbon in boron carbide, silicon carbide, and mixtures thereof *J. Less-Common Met.* **117** 7
[20] Gosset D and Colin M 1991 Boron carbides of various compositions: an improved method for x-rays characterization *J. Nucl. Mater.* **183** 161–73
[21] Kuhlmann U and Werheit H 1992 On the microstructure of boron carbide *Solid State Commun.* **83** 849
[22] Kuhlmann U, Werheit H and Schwetz K A 1992 Distribution of carbon atoms on the boron carbide structure elements *J. Alloys Compounds* **189** 249
[23] Werheit H, Au T, Schmechel R, Shalamberidze S O, Kalandadze G I and Eristavi A M 2000 IR active phonons and structure elements of isotope-enriched boron carbide *J. Solid State Chem.* **154** 79
[24] Werheit H, Rotter H W, Meyer F D, Hillebrecht H, Shalamberidze S O, Abzianidze T G and Esadze E G 2004 FT-Raman spectra of isotope-enriched boron carbide *J. Solid State Chem.* **177** 569–74
[25] Kwei G H and Morosin B 1996 Structures of the boron-rich boron carbides from neutron powder diffraction: implication for the nature of the inter-icosahedral chains *J. Phys. Chem.* **100** 8031–9
[26] Mauri F, Vast N and Pickard C J 2001 Atomic structure of icosahedral B_4C boron carbide from a first principles analysis of NMR spectra *Phys. Rev. Lett.* **87** 085506
[27] Werheit H, Kuhlmann U and Lundström T 1994 On the insertion of carbon atoms in B_{12} icosahedra and the structural anisotropy of β-rhombohedral boron and boron carbide *J. Alloys Compounds* **204** 197–208
[28] Werheit H, Schmechel R, Kuhlmann U, Kampen T U, Mönch W and Rau A 1999 On the reliability of the Raman spectra of boron-rich solids *J Alloys Compounds* **291** 28–32
[29] Devreese J T 2005 Polaron *Encyclopedia of Physics* vol 2, ed R G Lerner and G L Trigg (Weinheim: Wiley–VCH) pp 2004–27
[30] Geist D, Meyer J and Peussner H 1970 Electrical conductivity and movable carrier electron paramagnetic resonance (EPR) *Boron* vol 3, ed T Niemyski (Warszawa: PWN-Polish Scientific Publishers) pp 207–14
[31] Werheit H, Binnenbruck H and Hausen A 1971 Optical properties of boron carbide and comparison with β-rhombohedral boron *Phys. Status Solidi* b **47** 153–8
[32] Binnenbruck H and Werheit H 1979 IR-active phonons of boron and boron carbide *Z. Naturf.* a **34** 787–98
[33] Calandra M, Vast N and Mauri F 2004 Superconductivity from doping boron icosahedra *Phys. Rev.* B **69** 224505
[34] Schmechel R and Werheit H 1997 Evidence of the superposition of Drude type and hopping type transport in boron-rich solids *J. Solid State Chem.* **133** 335
[35] Schmechel R and Werheit H 1998 Dynamical transport in icosahedral boron-rich solids *J. Mater. Process. Manuf. Sci.* **6** 329–37

[36] Werheit H, Herstell B and Winkelbauer W 1990 unpublished results
[37] Butcher P N and Morris P L 1973 *J. Phys. C: Solid State Phys.* **6** 2147
[38] Wood C 1985 Transport properties of boron carbide *AIP Conf. Proc.* **140** 206–15
[39] Emin D 1993 Optical properties of large and small polarons and bipolarons *Phys. Rev.* B **48** 13691–702
[40] Schmechel R, Werheit H, Kueffel V and Lundström T 1997 *Proc. 16th Int. Conf. on Thermoelectrics (Dresden, Germany)* ed A Heinrich and J Schumann (Piscataway, NJ: IEEE) p 219 (97TH8291)
[41] Schmechel R and Werheit H 1996 On the dynamical conductivity in icosahedral boron-rich solids *J. Phys.: Condens. Matter* **8** 7263–75
[42] Chauvet O, Emin D, Forro L, Aselage T L and Zuppiroli L 1996 Spin susceptibility of boron carbides: dissociation of singlet small bipolarons *Phys. Rev.* B **53** 14450–7
[43] Werheit H, Kuhlmann U, Franz R, Winkelbauer W, Herstell B, Fister D and Neisius H 1991 Electronic transport properties of boron carbide within the homogeneity range *Boron-Rich Solids*; *AIP Conf. Proc.* **231** 104–7
[44] Werheit H, Franz R, Schneider D, Wolf M and Brann G 1987 Hall effect and magnetoresistance of single crystalline boron carbide in high magnetic fields *Proc. 9th Int. Symp. on Boron Borides and Rel. Comp.* ed H Werheit (Duisburg: University Press) pp 381–2
[45] Werheit H and Schmechel R 1999 Boron *Numerical Data and Functional Relationships in Science and Technology* (*Landolt–Börnstein New Series* Group III, vol 41C) ed O Madelung (Berlin: Springer) pp 1–148
[46] Werheit H and Moldenhauer A 2006 On the diffusion of free carriers in β-rhombohedral boron *J. Solid State Chem.* **179** 2775–8
[47] Holstein T 1973 *Phil. Mag.* **27** 225
[48] Emin D 1977 The sign of the Hall effect in hopping conduction *Phil. Mag.* **35** 1188
[49] Geist D, Meyer J and Peussner H 1970 Electrical conductivity and movable carrier electron paramagnetic resonance *Boron* vol 3, ed T Niemyski (Warszawa: PWN) pp 207–14
[50] Geist D 1977 Electron paramagnetic resonance (EPR) in boron nitride, boron and boron carbide *Boron and Refractory Borides* ed V I Matkovich (Berlin: Springer) pp 65–77
[51] Schmechel R, Werheit H, Kampen T U and Mönch W 2004 Photoluminescence in boron carbide *J. Solid State Chem.* **177** 566–8
[52] Feng Y, Seidler G T, Cross J O, Macrander A T and Rehr J J 2004 Role of inversion symmetry and multipole effects in nonresonant x-ray Raman scattering from icosahedral B_4C *Phys. Rev.* B **69** 125402
[53] Werheit H 2006 On excitons in boron carbide *J. Phys.: Condens. Matter* **18** 10655–62
[54] Werheit H, Laux M, Kuhlmann U and Telle R 1992 Optical interband transitions of boron carbide *Phys. Status Solidi* b **172K** 81–6
[55] Werheit H, Binnenbruck H and Hausen A 1971 Optical properties of boron carbide and comparison with β-rhombohedral boron *Phys. Status Solidi* b **47** 153